

**DOE-FIU SCIENCE & TECHNOLOGY WORKFORCE  
DEVELOPMENT PROGRAM**

**STUDENT SUMMER INTERNSHIP TECHNICAL REPORT**

June 4, 2012 to August 10, 2012

**Development of a Parallel, 3D, Lattice  
Boltzmann Method CFD Solver for  
Simulation of Turbulent Reactor Flow**

**Principal Investigators:**

Jaime Mudrich (DOE Fellow)  
Florida International University

Prashant Jain, Ph.D., Mentor  
Oak Ridge National Laboratory

**Acknowledgements:** Emilian Popov, Ph.D.  
Abhijit Joshi, Ph.D.

**Florida International University Program Director:**

Leonel Lagos Ph.D., PMP®

**Prepared for:**

U.S. Department of Energy  
Office of Environmental Management  
Under Grant No. DE-EM0000598

### **DISCLAIMER**

This report was prepared as an account of work sponsored by an agency of the United States government. Neither the United States government nor any agency thereof, nor any of their employees, nor any of its contractors, subcontractors, nor their employees makes any warranty, express or implied, or assumes any legal liability or responsibility for the accuracy, completeness, or usefulness of any information, apparatus, product, or process disclosed, or represents that its use would not infringe upon privately owned rights. Reference herein to any specific commercial product, process, or service by trade name, trademark, manufacturer, or otherwise does not necessarily constitute or imply its endorsement, recommendation, or favoring by the United States government or any other agency thereof. The views and opinions of authors expressed herein do not necessarily state or reflect those of the United States government or any agency thereof.

## ABSTRACT

---

The lattice Boltzmann method (LBM) is a relatively young (~20 years) computational fluid dynamics (CFD) algorithm, but has been proven to be a very effective fluid solver. LBM offers advantages over traditional Navier-Stokes equation solvers in the form of exceptional scalability, robust treatment of complex boundaries, and the capacity to take greater time steps. With such advantages in mind, the Thermal Hydraulics and Irradiation Engineering group of the Reactor and Nuclear Systems Division at Oak Ridge National Laboratory is developing a parallel, three-dimensional, LBM, CFD solver called PRATHAM with the intent of simulating fluid flow in a nuclear reactor. Several benchmark cases were examined with the PRATHAM solver to verify various aspects of the program and inspire confidence and acceptance as a CFD tool. Velocity and bounce-back boundary conditions were verified using the benchmark case of two-dimensional, lid-driven flow in a cavity. The body-force feature was verified using the case of two-dimensional, body-driven Poiseuille flow. The pressure (or density, as they are related by the equation of state in the LBM) was explored using the case of two-dimensional, pressure-driven Poiseuille flow. The benchmark for the pressure boundary condition was acceptable except for some deviant behavior at the boundaries.

## TABLE OF CONTENTS

---

ABSTRACT.....	iii
TABLE OF CONTENTS.....	iv
LIST OF FIGURES .....	v
1. INTRODUCTION .....	1
2. EXECUTIVE SUMMARY .....	2
3. RESEARCH DESCRIPTIONS .....	3
3.1 Velocity Boundary Condition Benchmarking .....	3
3.2 Forcing Term Benchmarking.....	5
3.3 Pressure/Density Boundary Condition Benchmarking .....	5
4. RESULTS AND ANALYSIS.....	6
4.1 Velocity Boundary Condition Benchmarking .....	6
4.1.1 Case 1: $Re = 1,000$ .....	6
4.1.2 Case 2: $Re = 5,000$ .....	8
4.1.3 Case 3: $Re = 10,000$ .....	10
4.2 Forcing Term Benchmarking.....	11
4.3 Pressure/Density Boundary Condition Benchmarking .....	12
5. CONCLUSION.....	14
6. REFERENCES .....	15
APPENDIX A.....	16
A.1 Parameter Calculation for Forcing Term Benchmarking.....	16
A.2 Parameter Calculation for Pressure Boundary Condition Benchmark.....	17

## LIST OF FIGURES

---

Figure 1. Lid-driven cavity boundary conditions. ....	3
Figure 2. Steady-state solution for $Re = 1000$ , stream function illustrates flow for lid driven cavity simulation (1). ....	4
Figure 3. 2D body-driven Poiseuille flow boundary conditions and velocity profile. ....	5
Figure 4. 2D pressure-driven Poiseuille flow boundary conditions and velocity profile. ..	5
Figure 5. Vertical velocities taken from horizontal slice (left) Horizontal velocities taken from vertical slice (right). ....	6
Figure 6. Lid-driven cavity horizontal velocity results for $Re = 1000$ at 200000 ts. ....	7
Figure 7. Lid-driven cavity vertical velocity results for $Re = 1000$ at 200000 ts. ....	7
Figure 9. Lid-driven cavity vertical velocity results for $Re = 5000$ at 500000 ts. ....	9
Figure 10. Lid-driven cavity horizontal velocity results for $Re = 10000$ at 500000 ts. ....	10
Figure 11. Lid-driven cavity horizontal velocity results for $Re = 10000$ at 500000 ts. ....	10
Figure 12. Coordinate system for forcing term benchmark. ....	11
Figure 13. Error analysis for forcing term benchmark. (Data compared at 125 points. Not all shown here.) ....	12
Figure 14. Error for pressure boundary condition benchmark. (Data compared at 125 points. Not all shown.) ....	13

# 1. INTRODUCTION

---

Most of the leading three-dimensional (3D) computational fluid dynamics (CFD) software for turbulent flow simulations in geometries of practical interest solves the Reynolds-averaged Navier-Stokes (RANS) equation with closure turbulence models (e.g.,  $k$ - $\epsilon$ ,  $k$ - $\omega$ , low Reynolds number turbulence model). Though RANS-based turbulence models can provide a reasonably accurate time-averaged behavior for steady state flows, they usually fail to deliver the details and accuracy needed to follow a flow instability transient, model thermal striping physics or capture transient forcing terms in flow-induced structural vibrations in a nuclear reactor. Several persisting issues in other approaches for turbulent flow simulation [e.g., those related to parallel scalability and very fine grid requirements in large eddy simulation (LES) for incompressible flows] can be resolved by a new kinetic method called the lattice Boltzmann method (LBM), which has better algorithmic parallel scalability and can use a longer time step than Navier-Stokes equation (NSE)-based explicit solvers, resulting in a significant speedup and reduced wall-clock time for large simulations of practical interest.

At the Oak Ridge National Laboratory, efforts are under way to develop a 3D, parallel LBM code—called PRATHAM (**Pa**RAllel **T**hermal **H**draulic simulations using **A**dvanced **M**esosopic **M**ethods)—to demonstrate the accuracy and scalability of LBM for turbulent flow simulations in nuclear applications. The code has been developed using FORTRAN-90, and parallelized using the message passing interface MPI library. Silo library is used to compact and write the data files, and VisIt visualization software is used to post-process the simulation data in parallel. Both the single relaxation time (SRT) and multi relaxation time (MRT) LBM schemes have been implemented in PRATHAM. To capture turbulence without prohibitively increasing the grid resolution requirements, an LES approach is adopted, allowing large scale eddies to be numerically resolved while modeling the smaller (subgrid) eddies. In this work, a Smagorinsky model has been used, which modifies the fluid viscosity by an additional *eddy viscosity* depending on the magnitude of the rate-of-strain tensor. In LBM, this is achieved by locally varying the relaxation time of the fluid.

To gain support and acceptance for PRATHAM, it not only needs to illustrate the aforementioned advantages over traditional RANS-based turbulence models, but must also be competitive with respect to accuracy. To achieve this proof of accuracy, and so verify the algorithm, PRATHAM was used to simulate a series of widely accepted benchmark problems. The results from PRATHAM were compared with data from literature (1, 2) as well as analytical solutions.

## 2. EXECUTIVE SUMMARY

---

This research work has been supported by the DOE-FIU Science & Technology Workforce Initiative, an innovative program developed by the US Department of Energy's Office of Environmental Management (DOE-EM) and Florida International University's Applied Research Center (FIU-ARC). During the summer of 2012, a DOE Fellow intern (Jaime Mudrich) spent 10 weeks participating in a summer internship at Oak Ridge National Laboratory (ORNL) under the supervision and guidance of Dr. Prashant Jain. The intern's project was initiated on June 4, 2012, and continued through August 10, 2012 with the objective of assisting in the ongoing efforts in the development of the parallel, 3D, lattice Boltzmann method CFD fluid solver, PRATHAM, to be used for simulation of reactor flow.

### 3. RESEARCH DESCRIPTION

#### 3.1 Velocity Boundary Condition Benchmarking

To verify the velocity boundary conditions, simulations of a two-dimensional, shear-driven cavity were performed. For the case of  $Re = 1000$ , the results were compared to the collected data from Bruneau and Saad (1) that includes, among others, the traditionally referenced data of Ghia, Ghia and Shin (2). The cases of  $Re = 5000$  and  $Re = 10000$  were also simulated, but compared exclusively against the second reference (2).

The two-dimensional, shear-driven cavity case is illustrated in **Figure 1**. The domain is square. Three sides of the domain are walls with the no-slip boundary condition such that  $u = v = 0$ . The fourth side of the square has a specified velocity parallel to that side (hence shear-driven) and zero velocity in the orthogonal direction. **Figure 1** illustrates the system configuration. **Figure 2** illustrates the stream function for the steady solution of the lid-driven cavity simulation when  $Re = 1,000$ . The flow exhibits one large, central vortex and two secondary vortices in the corners opposite the velocity boundary.

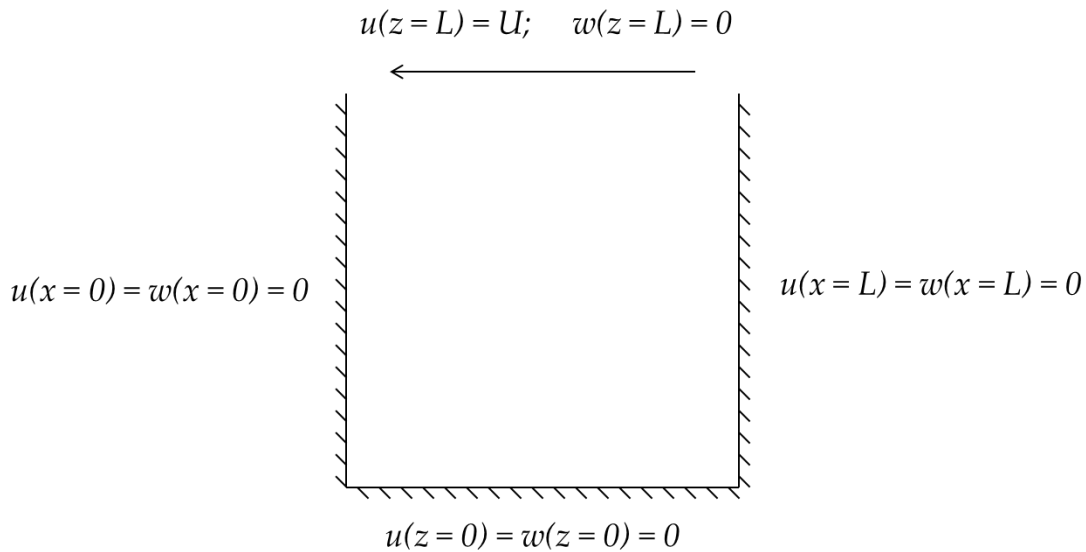


**Figure 1. Lid-driven cavity boundary conditions.**



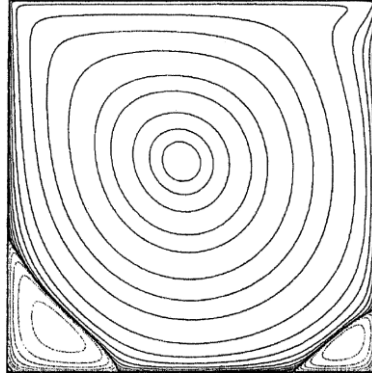


**Figure 2. Steady-state solution for  $Re = 1000$ , stream function illustrates flow for lid driven cavity simulation (1).**

### 3.2 Forcing Term Benchmarking

To verify the forcing term used to represent body forces such as gravity or the effects found in magneto hydrodynamics, the case of body-driven Poiseuille flow was simulated. This case is ideal because an analytical solution is available for comparison.

In this simulation, the fluid flows through a rectangular domain. The boundaries orthogonal to the direction of flow are periodic. The boundaries that are parallel to and confine the flow are no-slip, bounce-back boundaries. **Figure 3**, below, illustrates the system configuration and the steady-state velocity profile.

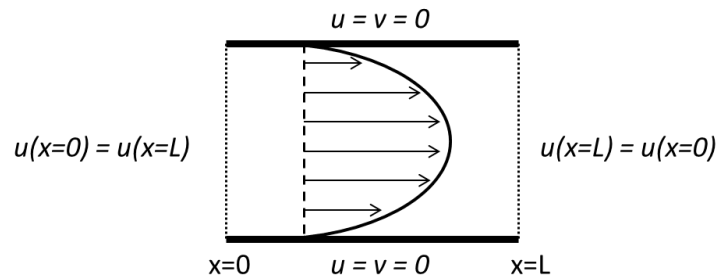


**Figure 3. 2D body-driven Poiseuille flow boundary conditions and velocity profile.**

### 3.3 Pressure/Density Boundary Condition Benchmarking

To verify the pressure/density boundary conditions, the case of pressure-driven Poiseuille flow was simulated. This case is ideal because an analytical solution is available for comparison.

In this simulation, the fluid flows through a rectangular domain. The boundaries orthogonal to the direction of flow are periodic. The boundaries that are parallel to and confine the flow are no-slip, bounce-back boundaries. **Figure 4**, below, illustrates the system configuration and the steady-state velocity profile.

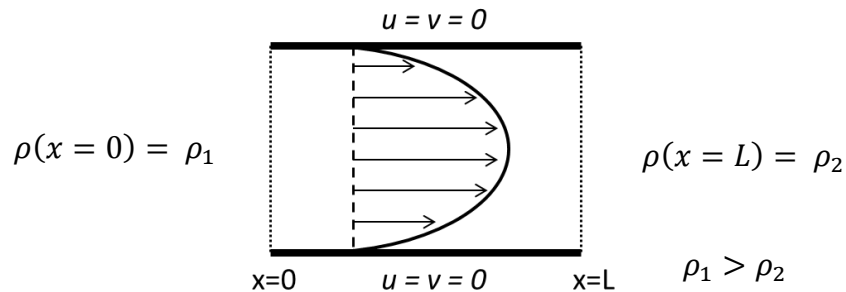


**Figure 4. 2D pressure-driven Poiseuille flow boundary conditions and velocity profile.**

## 4. RESULTS AND ANALYSIS

---

### 4.1 Velocity Boundary Condition Benchmarking

The data used to form the comparison between literature data and the PRATHAM simulation results was the velocity profile along two bisectors of the domain. The horizontal velocity,  $u$ , is taken across a vertical slice through the domain. The vertical velocity,  $v$ , is taken across a horizontal slice through the domain. **Figure 5** below illustrates the method in which data was collected for comparison.

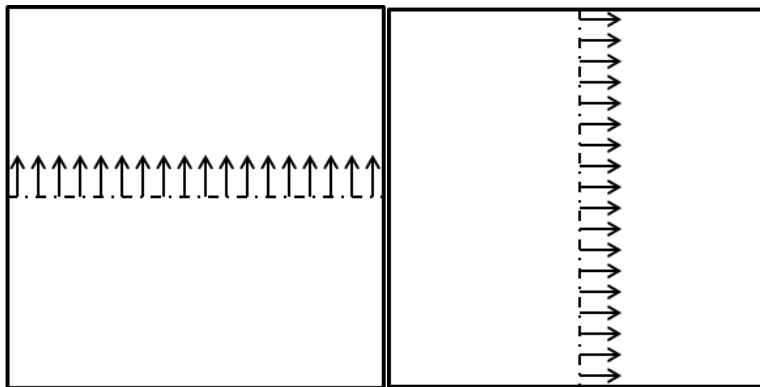


**Figure 5. Vertical velocities taken from horizontal slice (left) Horizontal velocities taken from vertical slice (right).**

#### 4.1.1 Case 1: Re = 1,000

First, the input parameters were calculated to give the correct Reynolds number, sufficient resolution and a physical relaxation time. The following illustrates the procedure.

$$Re = \frac{LU}{\nu} \rightarrow 1,000 = \frac{(200 \text{ } lu)(0.1 \text{ } lu \text{ } ts^{-1})}{\nu} \rightarrow \nu = 0.02 \text{ } lu^2 \text{ } ts^{-1}$$

“ $L$ ” is the length of the cavity and represents the resolution of the simulation. The value of  $200 \text{ } lu$  was selected initially for the length because it would provide good resolution and conserve computation time. Results show it is a suitable selection for this particular case. “ $U$ ” is the horizontal velocity of the lid and is set to  $0.1 \text{ } lu \text{ } ts^{-1}$ . “ $\nu$ ” is the kinematic viscosity of the fluid and is defined by the other two specified parameters as well as the Reynolds number defining the particular case. **Figure 6** and **Figure 7** below provide a comparison of the results from PRATHAM and those found in the first reference (1).

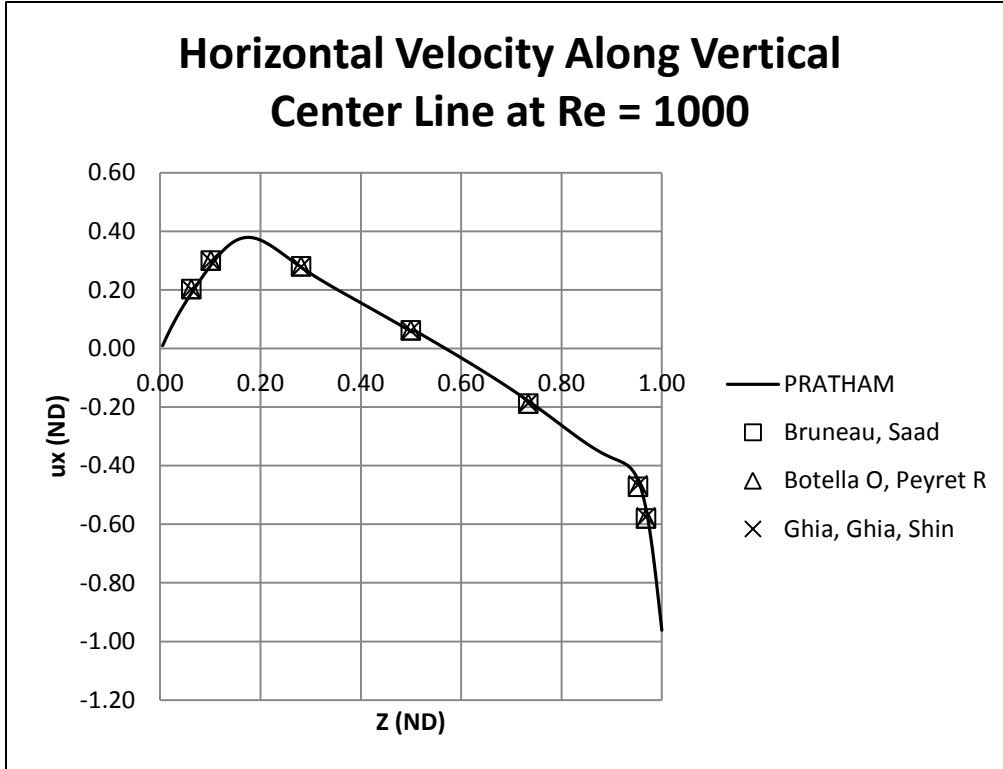


Figure 6. Lid-driven cavity horizontal velocity results for Re = 1000 at 200000 ts.

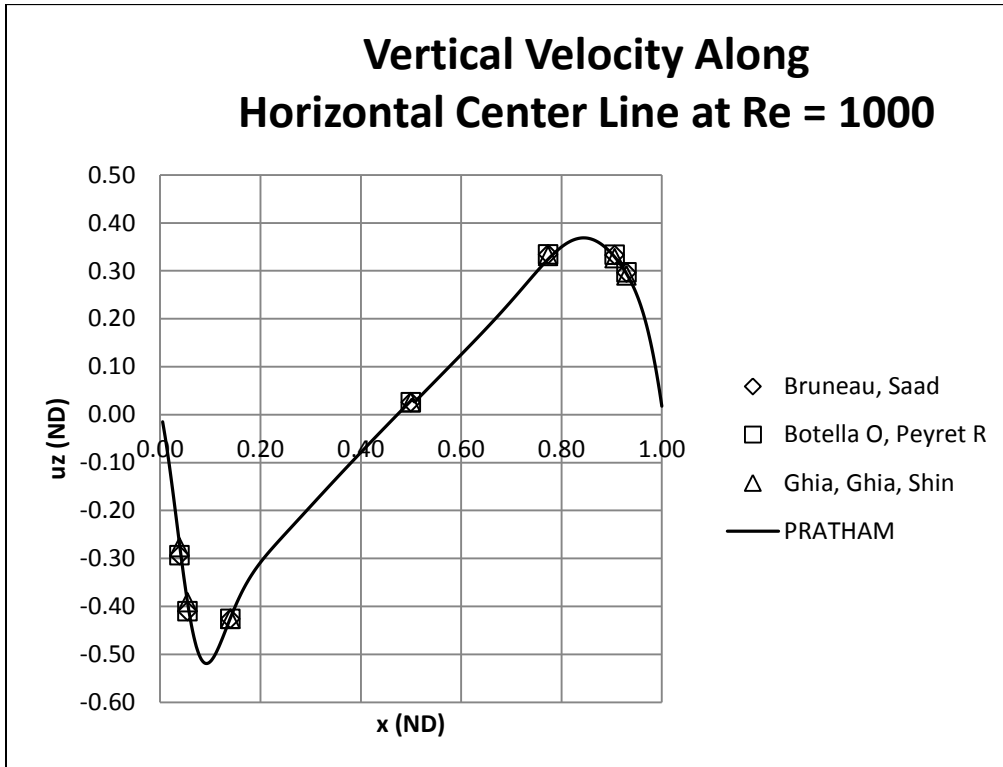


Figure 7. Lid-driven cavity vertical velocity results for Re = 1000 at 200000 ts.

From **Figure 6** and **Figure 7**, it is qualitatively clear that the results from PRATHAM are in good agreement with data from literature (1, 2). Quantitatively speaking, there is a maximum difference of three percent in the horizontal velocities and a maximum difference of two percent in the vertical velocities. These differences are acceptable on the basis that the PRATHAM simulation used only one fifth of the resolution of that in the first reference (1). These errors can be lessened by refining the mesh size and adjusting the kinematic viscosity accordingly.

**4.1.2 Case 2: Re = 5,000**

$$Re = \frac{LU}{\nu} \rightarrow 5,000 = \frac{(400 \text{ lu})(0.1 \text{ lu ts}^{-1})}{\nu} \rightarrow \nu = 0.008 \text{ lu}^2 \text{ ts}^{-1}$$

**Figure 8** and **Figure 9** below provide a comparison of the results from PRATHAM and those found in the second reference (2) at a Reynolds number of five thousand.

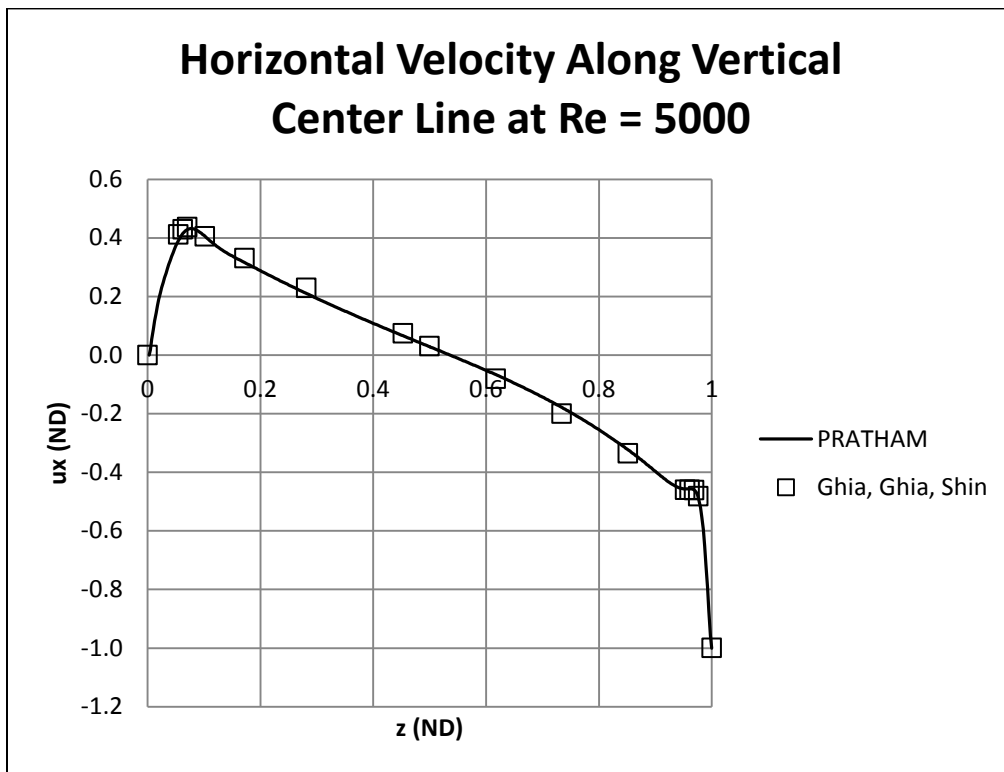


**Figure 8. Lid-driven cavity horizontal velocity results for Re = 5000 at 500000 ts.**

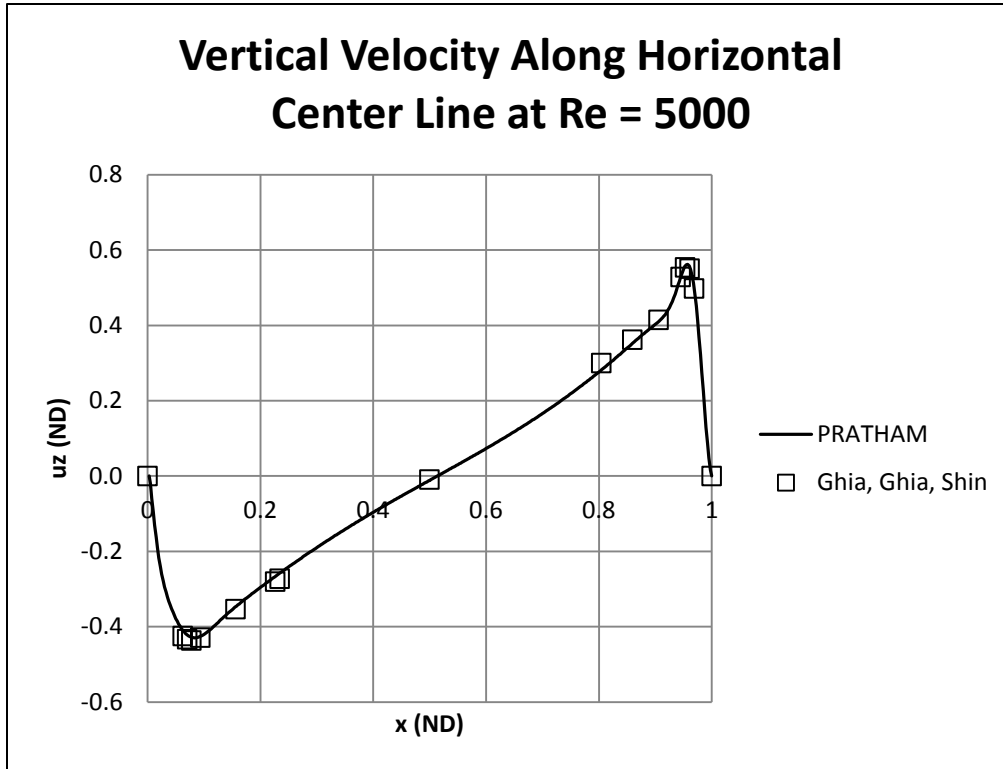


Figure 9. Lid-driven cavity vertical velocity results for Re = 5000 at 500000 ts.

From Figure 8 and Figure 9, it is qualitatively clear that the results from PRATHAM are in good agreement with data from literature (2). Quantitatively speaking, there is an average difference of five percent in the horizontal velocities and an average difference of four percent in the vertical velocities. These differences are acceptable on the basis that the PRATHAM simulation used only one fifth of the resolution of that in the second reference (2). These errors can be lessened by refining the mesh size and adjusting the kinematic viscosity accordingly.

**4.1.3 Case 3:  $Re = 10,000$**

$$Re = \frac{LU}{\nu} \rightarrow 10,000 = \frac{(400 \text{ lu})(0.1 \text{ lu ts}^{-1})}{\nu} \rightarrow \nu = 0.004 \text{ lu}^2 \text{ ts}^{-1}$$

Figure 10 and Figure 11 below provide a comparison of the results from PRATHAM and those found in the second reference (2) at a Reynolds number of ten thousand.

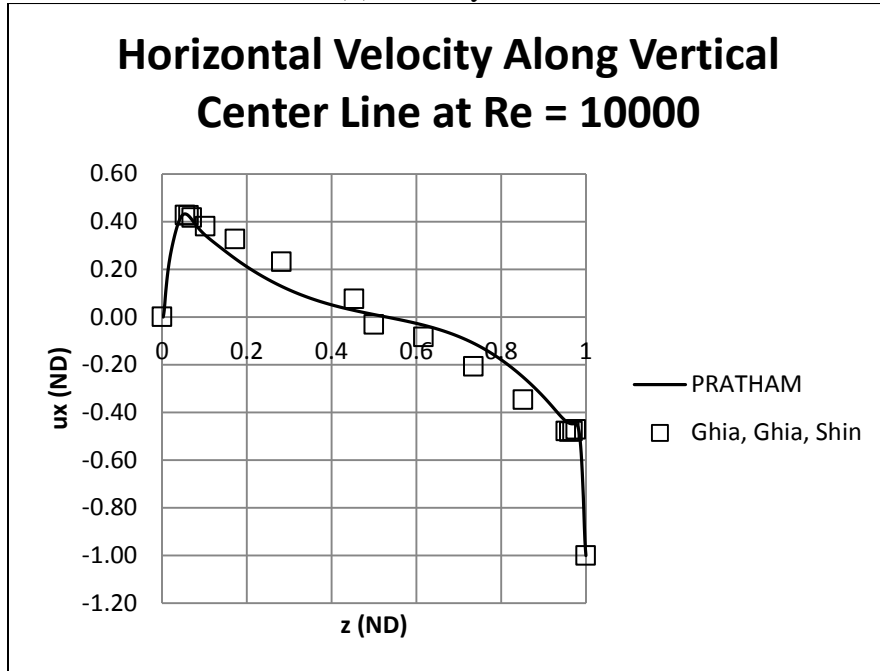


Figure 10. Lid-driven cavity horizontal velocity results for  $Re = 10000$  at 50000 ts.

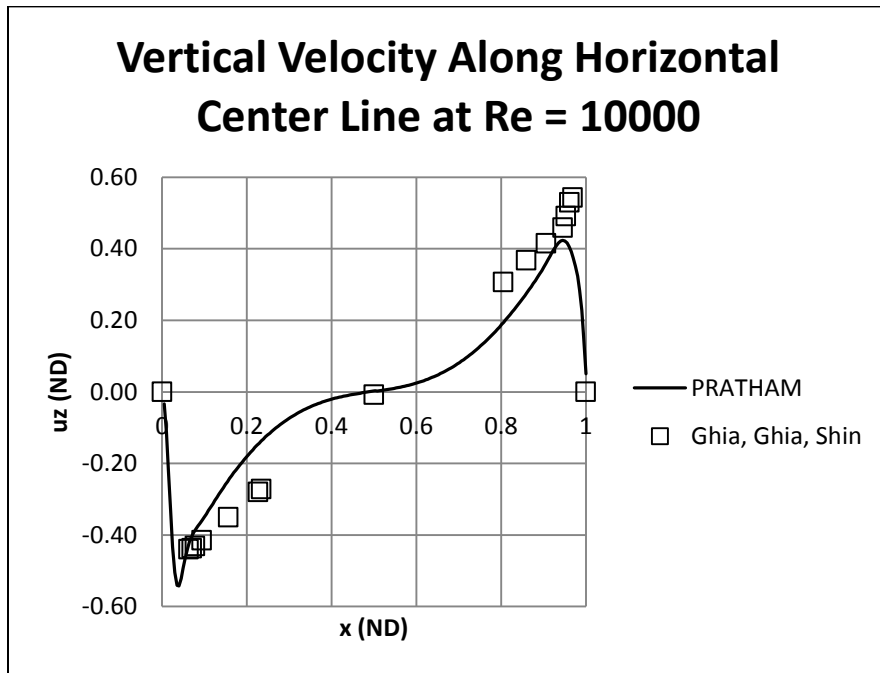


Figure 11. Lid-driven cavity horizontal velocity results for  $Re = 10000$  at 50000 ts.

Unlike the cases for  $Re = 1,000$  and  $Re = 5,000$ , the PRATHAM results for the two-dimensional lid-driven cavity benchmark at  $Re = 10,000$  is considerably out of agreement with the reference data in (2). It is suggested that the simulations be repeated with a finer mesh, closer to that described in the second reference (2). In the second reference (2), the mesh size is 1024 by 1024 non-dimensional units, but the PRATHAM simulation was performed on a mesh of only 400 by 400 non-dimensional units. The mesh discrepancy could be overlooked at lower Reynolds numbers, but **Figure 10** and **Figure 11** clearly show that the PRATHAM mesh must be refined and should more closely match the resolution of the second reference (2).

### 4.2 Forcing Term Benchmarking

To benchmark the forcing term, the case of two-dimensional Poiseuille flow was considered. This type of flow has an analytical solution that was used to calculate the error in the PRATHAM simulation. The equation below describes the velocity in the flow direction.

$$u(z) = \frac{G}{2\rho\nu} (a^2 - z^2)$$

Where  $G$  represents the hydraulic gradient,  $a$  represents the channel radius,  $\rho$  represents density,  $u$  represents the velocity in the x-direction and  $\nu$  represents kinematic viscosity. The calculations required to define the parameters  $a$ ,  $\rho$ ,  $\nu$ , and  $G$  are included in the appendix. **Figure 12** below illustrates the coordinate system for the benchmark.

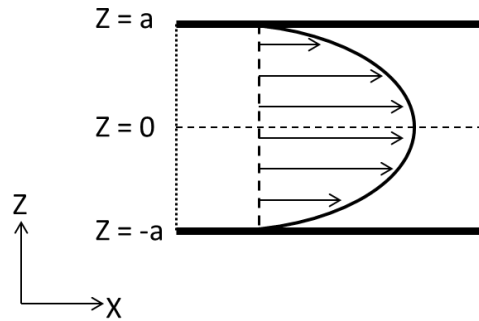


**Figure 12. Coordinate system for forcing term benchmark.**

The data used to form the comparison between analytical solution and the PRATHAM simulation results was the velocity profile along a vertical slice of the domain. The horizontal velocity,  $u$ , is taken across the channel at any position,  $x$ , throughout the domain (fully-developed flow,  $\frac{\partial u}{\partial x} = 0$ ). **Figure 13** below presents the results.



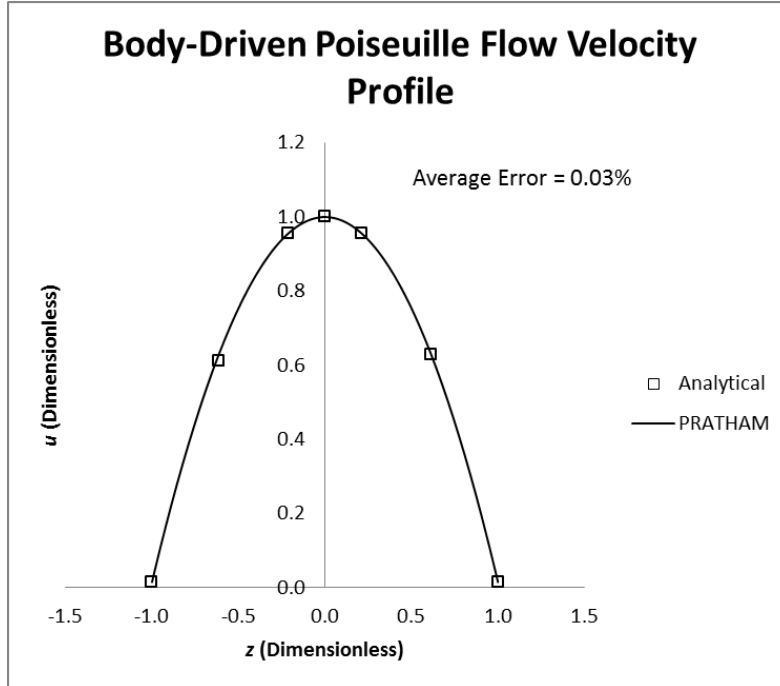


**Figure 13. Error analysis for forcing term benchmark. (Data compared at 125 points. Not all shown here.)**

From **Figure 13**, it is qualitatively clear that the results from PRATHAM are in good agreement with the analytical solution. Quantitatively speaking, there is an average relative error of three hundredths of a percent in the velocity profile. Such a minimal error serves to verify PRATHAM’s incorporation of the body force term.

### 4.3 Pressure/Density Boundary Condition Benchmarking

To benchmark the density/pressure (related by equation of state) boundary condition, the case of two-dimensional Poiseuille flow was considered. This type of flow has an analytical solution that was used to calculate the error in the PRATHAM simulation. The equation below describes the velocity in the flow direction.

$$u(z) = \frac{P_{in} - P_{out}}{2\rho_0\nu L} (a^2 - z^2)$$

Where  $P_{in/out}$  represents the inlet and outlet pressure respectively,  $a$  represents the channel radius,  $L$  represents the channel length,  $\rho_0$  represents a reference density,  $u$  represents the velocity in the x-direction and  $\nu$  represents kinematic viscosity. The calculations required to define the parameters  $a$ ,  $L$ ,  $\rho_0$ ,  $\nu$ , and  $P_{in/out}$  are included in the appendix. The coordinate system used for this benchmark is the same as for the problem in section 4.2 **Forcing Term Benchmarking** and can be seen in **Figure 12**. The results for this simulation are shown below in **Figure 14**.

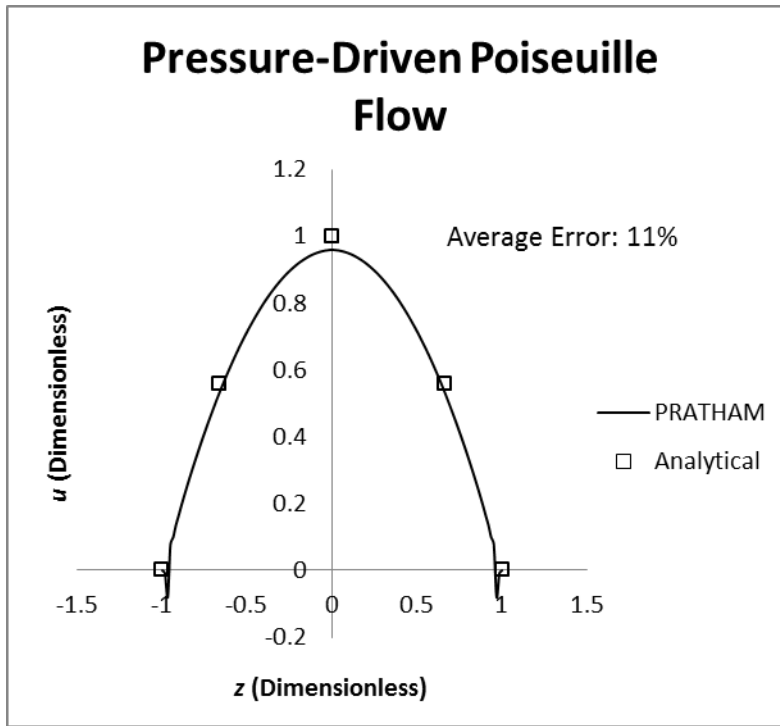


**Figure 14. Error for pressure boundary condition benchmark. (Data compared at 125 points. Not all shown.)**

From **Figure 14** above, it can be seen that the shape of the velocity profile is correct, but that there is a significant discrepancy between the analytical and simulated solutions. It should be noticed that the velocity,  $u$ , becomes negative near the boundaries of the channel ( $z = \pm 1$ ) which is not physical behavior for this system. From these observations, it seems that the pressure/density boundary conditions have been applied and are operating correctly, but the zero velocity boundaries at the walls are performing poorly. It should be noted that in this simulation, velocity boundaries were used on the walls instead of bounce-back boundaries as in the benchmark case of section 4.2

**Forcing Term Benchmarking**

## 5. CONCLUSION

---

The research at ORNL consisted of benchmarking efforts for the PRATHAM code. The features benchmarked include velocity boundary conditions, pressure/density boundary conditions and the forcing term.

The velocity boundary conditions were benchmarked accurately up to  $Re = 5,000$  and the case of  $Re = 10,000$  seems to only be in significant error because of discrepancy in mesh size between the literature values (2) and the PRATHAM simulation. It is recommended that the simulation for  $Re = 10,000$  be performed again with a finer mesh that more closely resembles the literature case.

The pressure/density boundary conditions were successfully benchmarked using the case of two-dimensional, pressure-driven Poiseuille flow. It was noted previously that there seems to be an issue with the velocity boundary conditions on the channel walls in this simulation which are causing a non-physical backward flow at the walls. The backward flow discrepancy should be examined further and identified as critical or negligible.

The forcing term was successfully benchmarked using the case of two-dimensional, body-driven Poiseuille flow. Minimal error throughout the entire velocity profile of the simulation results indicate that the forcing term is working correctly, the bounceback boundary condition is working correctly, and the periodic boundary condition is working correctly.

## 6. REFERENCES

---

1. *The 2D lid-driven cavity problem revisited*. Charles-Henri Bruneau, Mazen Saad. 2006, Elsevier, pp. 326-348.
2. *High-resolutions for incompressible flows using Navier-Stokes equations and a multigrid method*. Ghia U, Ghia KN, Shin CT. s.l. : J Comput Phys, 1982, Vol. 48.
3. *Pressure boundary condition of the lattice Boltzmann method for fully developed periodic flows*. Junfeng Zhang, Daniel Y. Kwok. s.l. : Physical Review E, 2006, Vol. 73.

## APPENDIX A.

---

### A.1 Parameter Calculation for Forcing Term Benchmarking

Symbol	Description	Units
$u_{max}$	Maximum Poiseuille flow velocity	$lu\ ts^{-1}$
$u_{avg}$	Average Poiseuille flow velocity	$lu\ ts^{-1}$
$\mu$	Dynamic viscosity	$mu\ lu^{-1}\ ts^{-1}$
$\nu$	Kinematic viscosity	$lu^2\ ts^{-1}$
$\rho_0$	Reference density	$mu\ lu^{-3}$
$\tau$	Relaxation time	$ts$
$Re$	Reynolds number	Dimensionless
$w$	Channel width	$lu$
$G$	Hydraulic gradient	$mu\ lu^{-2}\ ts^{-2}$

$$u_{max} = 0.1\ lu\ ts^{-1} \rightarrow u_{avg} = \frac{2}{3}u_{max} = 0.0\bar{6}\ lu\ ts^{-1}$$

$$\nu = \frac{1}{3}\left(\tau - \frac{1}{2}\right)$$

$$\tau = 1 \rightarrow \nu = \frac{1}{6}\ lu^2\ ts^{-1}$$

$$Re = \frac{u_{avg}w}{\nu} \rightarrow 50 = \frac{(0.0\bar{6}\ lu\ ts^{-1})w}{(0.1\bar{6}\ lu^2\ ts^{-1})} \rightarrow w = 125\ lu$$

$$u(z) = \frac{G}{2\mu}(a^2 - z^2)$$

$$\mu = \nu\rho$$

$$\rho_0 = 1\ mu\ lu^{-3}$$

$$\nu = \frac{1}{6}\ lu^2\ ts^{-1}$$

$$u_{max} = u(0) = \frac{G}{2\mu}a^2 = \frac{G}{\frac{1}{3}\ mu\ lu^{-1}\ ts^{-1}}a^2$$

$$a = \frac{1}{2}w = 62.5\ lu$$

$$u_{max} = G(3\ mu^{-1}\ lu\ ts)a^2 \rightarrow 0.1\ lu\ ts^{-1} = G(3\ mu^{-1}\ lu\ ts)(62.5\ lu)^2$$

$$G = 8.5\bar{3} * 10^{-6} \text{ mu lu}^{-2} \text{ ts}^{-2}$$

## A.2 Parameter Calculation for Pressure Boundary Condition Benchmark

$$u_{max} = 0.1 \text{ lu ts}^{-1} \rightarrow u_{avg} = \frac{2}{3} u_{max} = 0.0\bar{6} \text{ lu ts}^{-1}$$

$$\nu = \frac{1}{3} \left( \tau - \frac{1}{2} \right)$$

$$\tau = 1 \text{ ts} \rightarrow \nu = \frac{1}{6} \text{ lu}^2 \text{ ts}^{-1}$$

$$Re = \frac{u_{avg} w}{\nu} \rightarrow 50 = \frac{(0.0\bar{6} \text{ lu ts}^{-1}) w}{(0.1\bar{6} \text{ lu}^2 \text{ ts}^{-1})} \rightarrow w = 125 \text{ lu}$$

$$u(z) = \frac{P_{in} - P_{out}}{2\rho_0 \nu L} (a^2 - z^2) \rightarrow \frac{\rho_{in} - \rho_{out}}{3 \text{ lu}^{-2} \text{ ts}^2 * 2\rho_0 \nu L} (a^2 - z^2) \rightarrow$$

$$\rho_0 = 1 \text{ mu lu}^{-3}$$

$$\nu = \frac{1}{6} \text{ lu}^2 \text{ ts}^{-1}$$

$$u_{max} = u(0) = \frac{\rho_{in} - \rho_{out}}{6 \text{ lu}^{-2} \text{ ts}^2 * \rho_0 \nu L} a^2 = \frac{\rho_{in} - \rho_{out}}{1 \text{ mu lu}^{-3} \text{ ts} * L} a^2$$

$$a = \frac{1}{2} w = 62.5 \text{ lu}$$

$$u_{max} = 0.1 \text{ lu ts}^{-1} = \frac{(\rho_{in} - \rho_{out})(1 \text{ mu}^{-1} \text{ lu}^3 \text{ ts}^{-1}) a^2}{L} \rightarrow$$

$$0.1 \text{ lu ts}^{-1} = \frac{(\rho_{in} - \rho_{out})(1 \text{ mu}^{-1} \text{ lu}^3 \text{ ts}^{-1})(62.5 \text{ lu})^2}{L}$$

$$\frac{(\rho_{in} - \rho_{out})}{L} = 2.5\bar{6} * 10^{-5} \text{ mu lu}^{-4}$$

$$L = 700 \text{ lu} \rightarrow \rho_{in} - \rho_{out} = 0.01792 \text{ mu lu}^{-3}$$

$$\rho_{in} = 1.005973 \text{ mu lu}^{-3} \rightarrow \rho_{out} = 1.000000 \text{ mu lu}^{-3}$$